Characteristics of radio-loud CMEs

Conference Paper · August 2016

DOI: 10.1109/URSIAP-RASC.2016.7883559

Pankaj Kumar

NASA Goddard Space Flight Center, Greenbelt, …

Kyungsuk Cho

Korea Astronomy and Space Science Institute

Characteristics of Radio-Loud CMEs

Pankaj Kumar
Korea Astronomy and Space Science Institute (KASI)
Daejeon, 305-348, Republic of Korea
Email: pankaj@kasi.re.kr

P.K. Manoharan
Radio Astronomy Centre, NCRA-TIFR
Udhagamandalam (Ooty)-643 001, India

K.S. Cho
Korea Astronomy and Space Science Institute (KASI)
Daejeon, 305-348, Republic of Korea

***Abstract*—In this paper, we study the characteristics of 46 radio-loud (RL) Coronal Mass Ejections (CMEs), which occurred during 1997-2006. All these RL CMEs were associated with M- and X-class flares. We selected 46 RL CMEs, out of which 26 events (57%) were associated with Solar Energetic Particle (SEP) events detected at 1 AU. Furthermore, we study the link between the flare accelerated electrons in the low corona and protons at 1 AU and found a positive correlation (30%). It suggests the link between the injection sites for electrons and protons, which are most likely accelerated at the flare current sheet. We also study the relation between the CME speed and peak proton flux (>10 MeV) at 1 AU and found a good correlation (∼60%), which suggests the proton acceleration by CME driven shocks. In addition, we found two branches (lower and upper) of SEP events with different characteristics. The lower branch SEP events are associated with impulsive rise along with more proton flux whereas the upper branch SEP events exhibit gradual rise and less proton flux. We suggest that flares (current sheet) and CMEs (shocks) both are involved in the particle acceleration for the lower branch, whereas in the upper branch mostly CME driven shocks play an important role in the particle acceleration.**

I. Introduction

Radio-loud (RL) CMEs are generally associated with intense radio bursts (i.e., type II, type III and type IV) . These are fast and wide CMEs, i.e. speed $\geq$400 km s^{-1} and width $\geq$100°. These are often associated solar energetic particle (SEP) events, with a proton intensity in the $\geq$10 MeV GOES channel $\geq$10 pfu (particle flux unit), 1 pfu = 1 particle cm^{-2} s^{-1} sr^{-1}.

SEPs can be originated by two processes: (i) acceleration at the solar flare current sheet (ii) by shock waves driven by CMEs. SEP events are subdivided into two categories: impulsive and gradual events. The later type is normally associated with CME-driven shocks during their propagation from solar corona to the interplanetary medium [1,2,3]. SEPs detected at 1 AU indicate magnetic connectivity between the flare/CME site and satellite, a necessary condition for particle propagation path. CME driven shocks accelerate at least two different seed populations, flare supra-thermals as well as solar-wind particle [4]. A correlation between the peak fluxes of SEPs and soft X-rays has been reported by some authors [5], which is well improved if we consider the SEP events in the western hemisphere [6]. Kiplinger et al. [7] has also reported that there is a high correlation between the 10 MeV proton flux at 1 AU and a characteristic pattern of X-ray spectral evolution of 18 flares. Chertok et al. [8] also found the existence of a statistical correspondence between the frequency spectra of solar microwave bursts and the energy spectra of near-Earth proton fluxes at the energies of tens of MeV. Therefore, it is still under debate whether the SEPs are purely associated with CME-driven shocks and/or there is some contribution from flares (current sheet) also.

In this paper, we analysed 46 radio-loud CMEs, associated SEP events, and investigated their characteristics. In section 2, we present the observational characteristics of RL CMEs and associated SEP events. In the last section, we summarize the results.

II. Observations and Results

The data sets utilized in this study are given below:
(i) We used radio flux 1-sec cadence data from the NGDC (National Geophysical Data Center) RSTN (Radio Solar Telescope Network) network to select the radio-loud CME events during 1997-2006 (ftp://ftp.ngdc.noaa.gov/STP/space-weather/solar-data/solar-features/solar-radio/rstn-1-second/).
(ii) We used LASCO C2 and C3 data for the CMEs characteristics (http://cdaw.gsfc.nasa.gov/CME _list/).
(iii) We utilized SOHO/EIT Extreme-ultraviolet images for coronal measurements and SOHO/MDI magnetogram data for the morphology of the active regions.
(iv) We used GOES proton flux (>10 MeV) data observed at 1 AU (http://spidr.ngdc.noaa.gov/spidr).
(v) We used coronal and interplanetary radio spectrum data from ground based (Learmonth and Culgoora radio observatories, ftp://ftp.ips.gov.au/wdc-data/spec/data/) and space-borne instrument (i.e. Wind/WAVES, http://www-lep.gsfc.nasa.gov/waves/waves.html).

First of all, we selected all the M- and X-class flare events during 1997-2006 using the flare lists from the NGDC. Then, we selected the radio-loud CME events comparing RSTN network radio flux density (sfu) in three different radio frequencies (245, 410, and 610 MHz, flux>1×10^5 sfu) with the SOHO/LASCO CME catalog. Fig. 1 shows the distribution of RL CMEs in three different radio frequencies (245, 410, and 610 MHz) during 1997-2006. These bar plots show that the number of events decreases with increasing frequency. It indicates that energy build-up and release process is different for different events which depends on the magnetic field configuration in the active region. Bottom left image shows the location of 46 radio-loud CMEs, out of which 26 CMEs

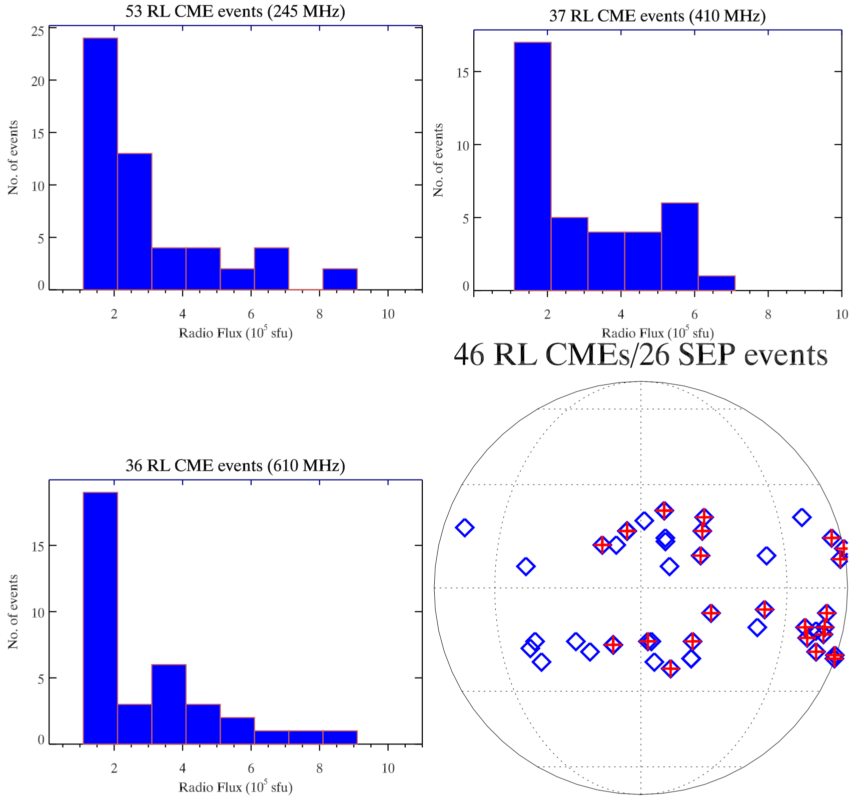

Fig. 1. Distribution of RL CMEs in three different radio frequencies (245, 410, and 610 MHz) during 1997-2006. The bar plots show that the number of events decreases with increasing frequency. Bottom-right image shows the location of 46 radio-loud CMEs, out of which 26 CMEs are associated with SEP events. **'+'** red symbols indicate the location of SEP events, whereas blue diamonds show the location of RL CME events . Most of the SEP events originate from the western hemisphere due to a favorable magnetic connectivity to the satellite.

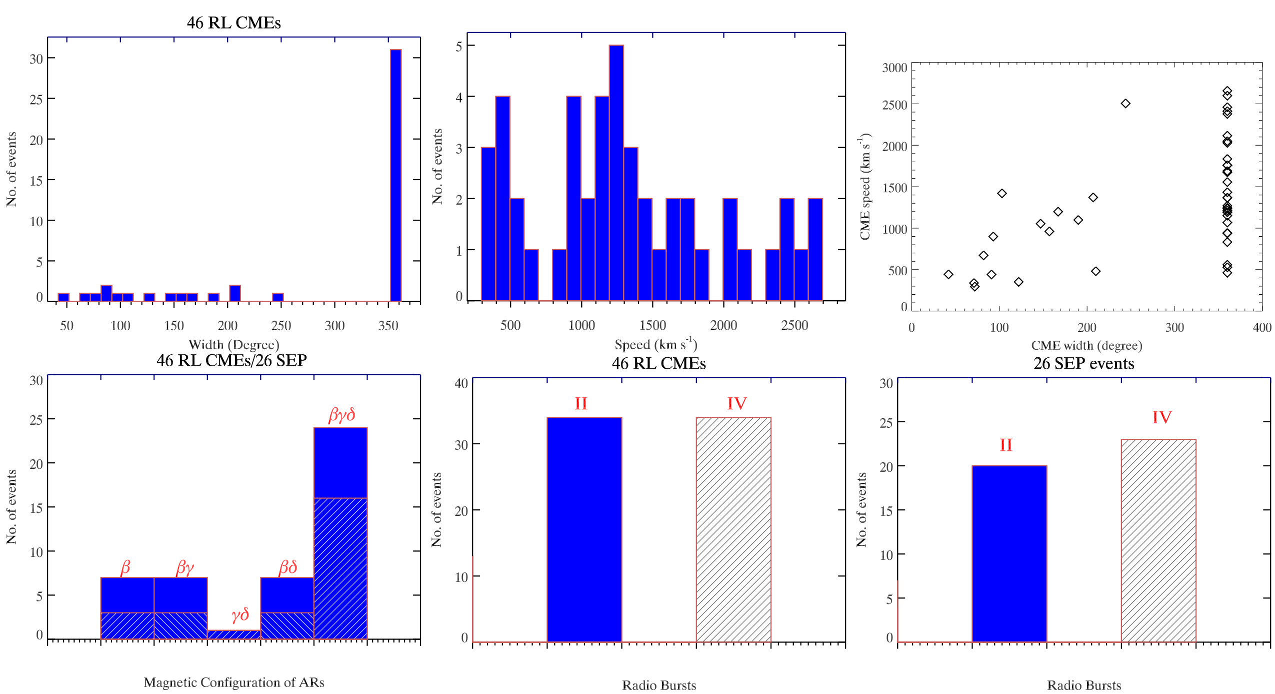

Fig. 2. Top: distribution of angular width, speed, and width vs. speed for the 46 RL CMEs. Bottom-left: Magnetic configuration of ARs associated with 46 Radio loud CMEs and 26 SEP events. Bottom-middle: Type II and Type IV radio bursts associated with RL CMEs. Bottom-right: Type II and Type IV radio bursts associated with SEP productive CMEs.

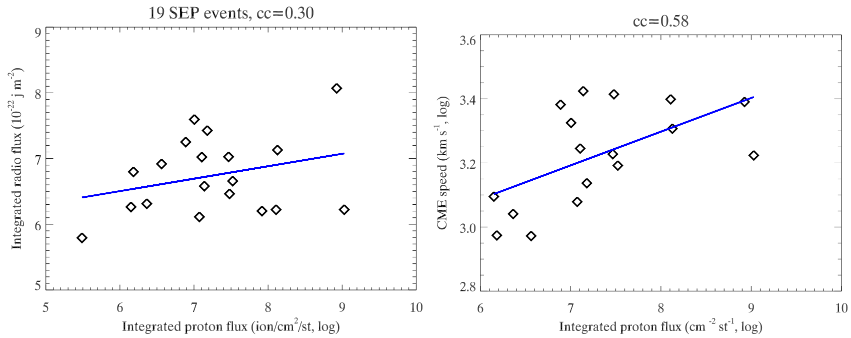

Fig. 3. Left: Integrated radio flux vs. integrated proton flux profile for 19 SEP events. Right: CME-speed vs. integrated proton flux profile for the same 19 events. 'cc' denotes the coefficient of correlation.

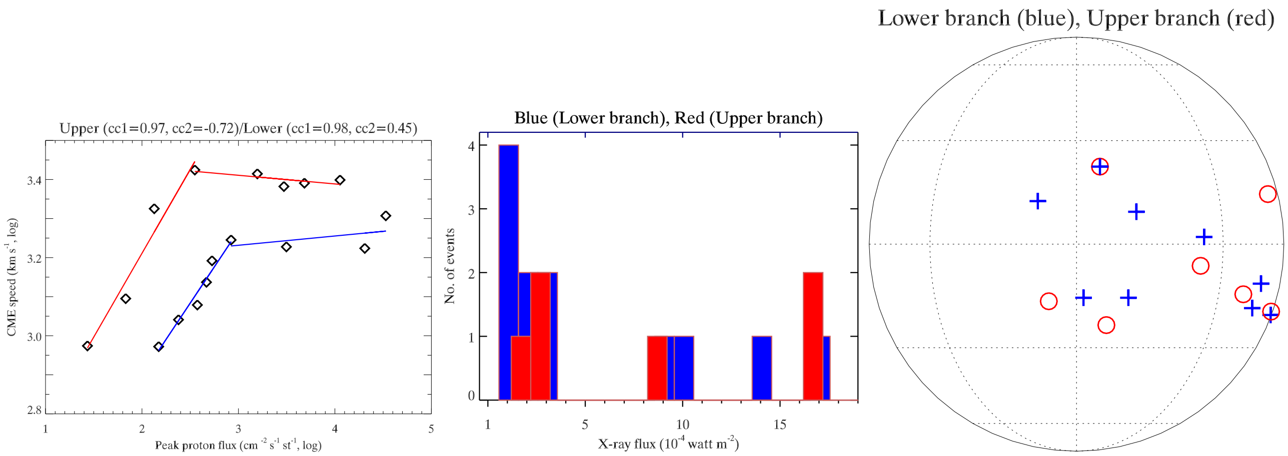

Fig. 4. Left: Peak proton flux observed at 1 AU by GOES vs. CME speed. It shows two separate groups/branches. Middle: Flare classification for these events. Right: Location of these events on the solar disc.

are associated with SEP events. **'+'** red symbols indicate the location of SEP events, whereas blue diamonds show the location of RL CME events . Most of the SEP events originated from the western hemisphere due to the favorable magnetic connectivity to the satellite. We selected 46 RL CME events for the detailed multiwavelength investigations regarding the characteristics of these CMEs.

Fig. 2 displays some of the characteristics of 46 RL CMEs. The top-left bar plot shows the width distribution of theses CMEs. This plot reveals that most of the RL CMEs are halo events ($\sim$70%) and remaining are also broad (e.g., partial halo CMEs). The top-middle bar plot shows the speed distribution of these CMEs. It shows that most of the radio loud CMEs are high speed CMEs (speed$\geq$400 km s^{-1}, median=1300 km s^{-1}). The CMEs width vs. speed has been plotted in the top-left panel, which shows that all halo CMEs have speeds 500–2700 km s^{-1}, whereas other CMEs have speed $<$1500 km s^{-1}. It may be noted that RL CMEs have large width, higher speed, and more kinetic energy.

The bottom-left plot displays the magnetic configuration of the ARs of 46 RL CMEs, which reveals that $\sim$52% RL CMEs events are associated with $\beta\gamma\delta$ magnetic configuration of the active region, whereas $\sim$62% SEP events are associated with $\beta\gamma\delta$ configuration. This indicates that complex ARs have more probability to produce the RL CMEs. The bottom-left bar plot shows the radio bursts (Type II and Type IV) associated with 46 RL CMEs. Out of these CMEs, $\sim$76% CMEs are associated with type II and type IV radio bursts, whereas other RL CME events do not show clear type II and type IV bursts. Further, out of 26 SEP events $\sim$80% CMEs show association with type II and type IV whereas other SEP events do not show clear type II and type IV radio bursts.

To determine the relationship between flare generated radio emission (due to accelerated electrons in the low corona) and protons at 1 AU, We estimate integrated radio flux density in three frequencies (245/410/610 MHz, in which CME is radio-loud) and the proton flux at 1 AU for 19 SEP events. The bottom-left plot shows the positive ($\sim$30%) correlation between these integrated flux profiles. It indicates that there may be common injection site (current sheet) for electrons and protons in the corona. The particle injection sites may vary for event to event depending on the magnetic field configuration of the ARs, which is in agreement with the earlier study [9,10]. The right panel of Fig. 3 shows the integrated proton flux [log(F)] vs. CME speed [log(V)] in the LASCO field of view. This plot shows good correlation ($\sim$58%) between these two parameters, which suggests that CMEs are the main driver for proton acceleration in the interplanetary medium.

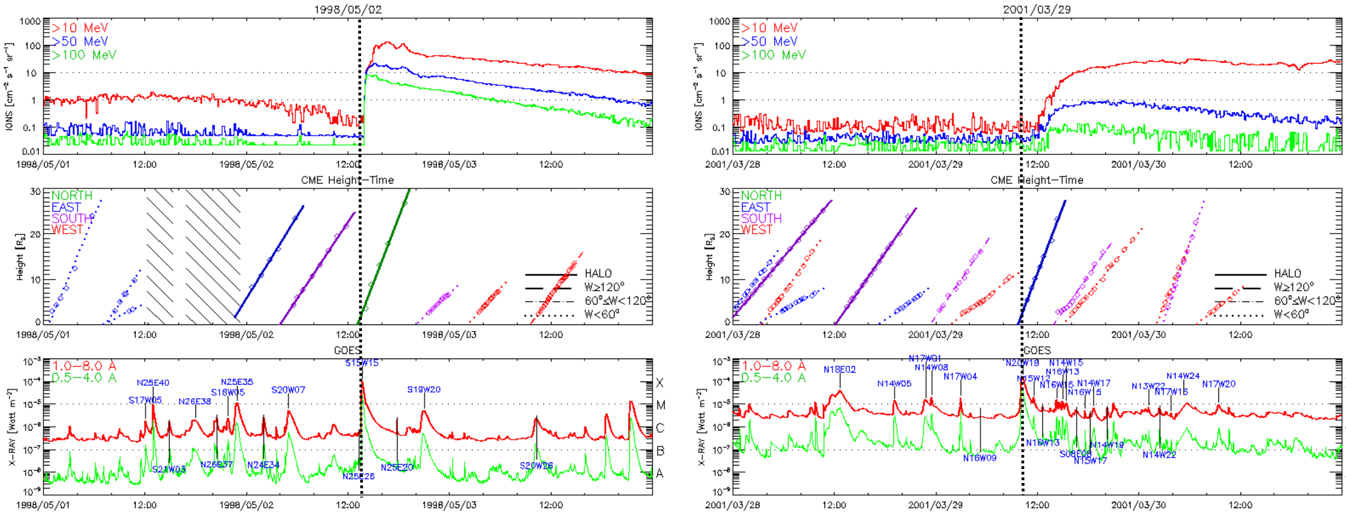

Fig. 5. Left: GOES soft X-ray, LASCO CME height-time and proton flux profiles at 1 AU for 2 May 1998 event (Lower-branch event). Right: The similar plots for 29 March, 2001 event (Upper branch event).

TABLE I
EVENTS SUMMARY

Events	location	CME speed	Flare	proton flux (pfu)
02 May 1998	15S 15W	938 km s^{-1}	X1.1	$\sim$100
29 March 2001	06N 37W	942 km s^{-1}	X1.2	$\sim$20

To study the role of CMEs in producing the SEPs, we plotted the peak proton flux [log(F_{peak})] and CME speed [log(V)] for these SEP events (Fig. 4). We used the peak proton flux since the flux is peaked when the SEPs have well connectivity to satellite at 1 AU. Interestingly, this plot separates the SEP events into two groups/branches. There is linear relation between peak proton flux and CME speed [f(t)$\sim V^{0.4}$]. In these groups of CMEs, two CMEs with different speeds produced almost same proton flux, whereas two CMEs of same speed also associated with different proton flux. We carefully analysed these events and found that all SEP events were associated with X-class flares as shown by the bar plot in the middle panel. We plotted the location of these events on the solar disc (right panel), which indicates that all these SEP events are located in the western hemisphere (i.e., well connected to the satellite).

Fig. 5 displays an example of two SEP events, one from the lower branch (02 May 1998) and another from the upper branch (29 March 2001). Both proton events were associated with almost similar CMEs (same speed) and X class flare. Moreover, both events were associated with type II and type IV radio bursts. The summary of these events is given below: We would like to know why two branches with similar CMEs show different proton flux. To answer this question, we compared proton flux profiles for all events and found that the lower branch SEP events show impulsive rise with larger proton flux whereas the upper branch SEP events reveal a gradual rise with lower proton flux. This behavior is shown in the example event (refer to Fig. 5).

III. Summary

We studied 46 RL CME events, which have larger width, speeds, and kinetic energy in comparison to the normal CMEs [9,10]. $\sim$57% of the RL CMEs were associated with SEP events. Radio emission from flare accelerated electrons and proton fluxes near 1 AU show a correlation of 30%, suggesting a common link between the injection sites (flare current sheet) for both electrons and protons. Interestingly, CME speed and peak proton flux showed two separate branches and their correlation. The lower branch proton flux profiles reveal the impulsive rise with higher proton flux, whereas the upper branch exhibits gradual rise with lower proton flux. We suggest that the flares (current sheet) and CME driven shocks contribute to the lower branch (hybrid) whereas in the upper branch CME driven shocks play main role in the particle acceleration. Radio-loudness may be used as a signal for the forecasting of SEP events, which could be very useful in the prediction of space weather events [11,12].

References

[1] D. Reames, Space Science Reviews vol. 90, pp. 413, 1999.
[2] S. W. Kahler, J. Geophys. Res. vol. 106, pp. 20947, 2001.
[3] P. K. Manoharan and G. Agalya, Advances in Geosciences vol. 27, pp. 165, 2011.
[4] M. Aschavanden, Space Science Reviews vol. 124, pp. 361, 2006.
[5] N. Gopalswamy, S. Yashiro, S. Krucker, G. Stenborg and R. A. Howard, Journal of Geophysical Research (Space Physics) vol. 109, pp. 12105, 2004.
[6] A. Belov, V. Kurt, H. Mavromichalaki and M. Gerontidou, Sol. Phys. vol. 246, pp. 457, 2007.
[7] A. L. Kiplinger, ApJ vol. 453, pp. 973, 1995.
[8] I. M. Chertok, V. V. Grechnev and N. S. Meshalkina, Astronomy Reports vol. 53, pp. 1059, 2009.
[9] G. Michalek, N. Gopalswamy and H. Xie, Sol. Phys. vol. 246, pp. 409, 2007.
[10] N. Gopalswamy, S. Yashiro, H. Xie, et al. ApJ, vol. 674, pp. 560-569, 2008
[11] K. Klein and G. Trottet, Space Sc. Rev. vol. 95, pp. 215, 2001.
[12] K. Klein, G. Trottet and A. Klassen, Sol. Phys., vol. 65, 2010.